
Listen to Interpret: Post-hoc Interpretability for Audio Networks with NMF

Anonymous Author(s)

Affiliation

Address

email

Abstract

1 This paper tackles *post-hoc* interpretability for audio processing networks. Our goal
2 is to interpret decisions of a trained network in terms of high-level audio objects
3 that are also listenable for the end-user. To this end, we propose a novel interpreter
4 design that incorporates non-negative matrix factorization (NMF). In particular,
5 a regularized interpreter module is trained to take hidden layer representations
6 of the targeted network as input and produce time activations of pre-learned NMF
7 components as intermediate outputs. Our methodology allows us to generate
8 intuitive audio-based interpretations that explicitly enhance parts of the input signal
9 most relevant for a network’s decision. We demonstrate our method’s applicability
10 on popular benchmarks, including a real-world multi-label classification task.

11 1 Introduction

12 Deep learning models, while state-of-the-art for several tasks in domains such as computer vision,
13 natural language processing and audio, are typically not interpretable. Their increasing use, especially
14 in decision-critical domains, necessitates interpreting their decisions. A good interpretation is often
15 characterized by its understandability for the end users (see for instance [16]). More importantly,
16 attributes that aid understandability may largely be dependent on the data modality. In this paper, our
17 aim is to generate *post-hoc* human-understandable interpretations for deep networks that process the
18 audio modality. Here, *post-hoc* interpretability refers to the problem of interpreting decisions of a
19 fixed pre-trained network.

20 Traditional approaches generate interpretations through input attribution, either directly on the
21 raw input features or on a given simplified representation [30, 37, 35, 27]. To generate more
22 understandable interpretations, a small number of approaches consider other means, such as logical
23 rules [36], sentences [19] and high-level concepts [15].

24 Most existing *post-hoc* interpretability methods are primarily designed for application to images and
25 tabular data. This limits their applicability to other data modalities such as audio. Although many
26 audio processing networks operate on spectrogram-like representations, which can be seen as 2D
27 time-frequency images, a visualization or attribution in this space is not as meaningful to a common
28 user as it is for images [26].

29 This leads us to build an interpretation system that takes into account audio-specific understandability
30 features. We motivate these features through an example: suppose an audio event detection network
31 deployed in a house recognizes an “alarm” sound event. An ideal interpreter for this classification
32 decision would have the ability to “show” that it was indeed an alarm sound that triggered this
33 decision. To do so, it must be able to localize the alarm amid other events in the house (for *e.g.* dog
34 barks, baby cries, background noise *etc.*) and make it listenable for the end-user. It is important to
35 highlight here the role of listenable interpretations for better understanding of an audio network’s
36 decisions – note that it would be much less meaningful for a human to see the alarm sound as

highlighted parts of a spectrogram. Thus making the following aspects important for our system design: (i) generating interpretations in terms of high-level audio objects that constitute a scene, (ii) segmenting parts of the input signal most relevant for a decision and providing it as listenable audio. It's worth emphasizing that audio interpretability is not the same as classical tasks of separation or denoising. These tasks involve recovering complete object of interest in the output audio. On the other hand, a classifier network might focus more on salient regions. When interpreting its decision and making it listenable we expect to uncover such regions and not necessarily the complete object of interest.

To this end, we propose a novel *post-hoc* interpreter for audio that employs a popular signal decomposition technique called Non-negative Matrix Factorization (NMF; Lee and Seung [25]). NMF seeks to decompose an audio signal into constituent spectral patterns and their temporal activations. Unlike principal component analysis, NMF is known to provide part-based decompositions [12]. Owing to these properties, we first use NMF to pre-learn a spectral pattern dictionary on our training data. This dictionary is then incorporated as a fixed decoder within our interpretation module. Specifically, we train our system to determine an intermediate encoding that performs two roles: (i) is able to reconstruct the input through the fixed NMF dictionary decoder, thus corresponding to time activations for dictionary components, (ii) at the same time, a function of this encoding is able to mimic the classifier's output. Training with these constraints allows us to generate, for any classifier decision, importance values over spectral patterns in our dictionary. Listenable interpretations are readily produced by inverting most important NMF spectral patterns back to the time domain.

In summary, we make the following contributions:

- We propose a novel NMF-based interpreter module for *post-hoc* interpretability that generates interpretations in terms of meaningful high-level audio objects, listenable for the end-user.
- We present an original formulation that constrains the interpreter encoding through two loss functions, one for input reconstruction through NMF dictionary and the other for fidelity to the network's decision. From a learning perspective, we show a new way to link NMF with deep neural networks, especially for generating interpretations.
- We extensively evaluate on two popular audio event analysis benchmarks, tackling both multi-class and multi-label classification tasks. The dataset for the latter is very challenging due to its collection in noisy real-world setting. Our method's design allows us to simulate feature removal and perform *faithfulness* evaluation.

2 Related Works

In this section, we position our work in relation to: (i) interpretability methods for audio, (ii) methods for concept-based interpretability and, (iii) use of NMF within the audio community, in particular, attempts to link it with deep networks.

Interpretability methods for audio Some approaches [5, 42] have shown usability of attention/visualization techniques for interpreting audio processing networks or generated instance-wise feature importance [44] for time-series data [39]. However, we focus here more on methods that attempt to address audio interpretability beyond image-based visualizations or raw input attribution. A few works have applied the popular LIME algorithm with a simplified input representation more suited for audio. In particular, SLIME [28, 29] proposes to segment the input along time or frequency. The input is perturbed by switching "on/off" the individual segments. AudioLIME [18, 10] proposes to separate input using predefined sources to create the simplified representation. AudioLIME arguably generates more meaningful interpretations than SLIME as it relies on audio objects readily listenable for end-user. However, it can only be applied for limited applications as it requires existence of known and meaningful predefined sources that compose the input audio. APNet [45] takes another promising direction by extending interpretable prototypical networks for audio input. However, they propose an interpretable system *by-design*. They don't tackle the problem of *post-hoc* interpretation.

Concept-based interpretability Our method relies on high-level objects for interpretation. In this sense, it is most closely related to *post-hoc* concept-based methods [21, 15]. An interesting approach is that of *post-hoc* version of FLINT [31] with whom we share the idea of utilizing the hidden layers and loss functions to encourage interpretability. However we crucially differ from

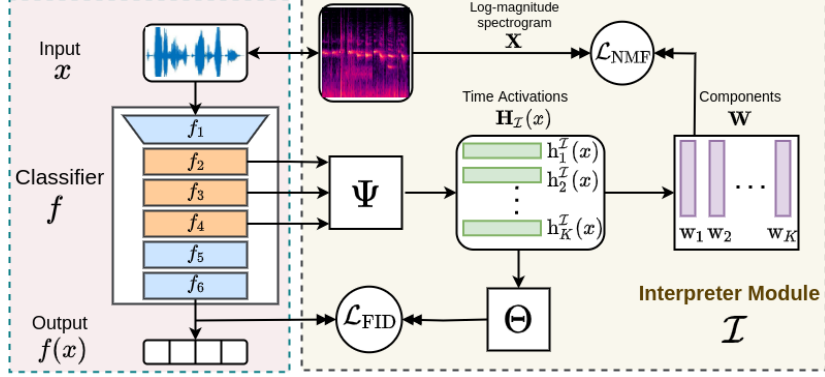


Figure 1: **System overview:** The interpretation module (right block) accesses hidden layer outputs of the network being interpreted (left block). These are used to predict an intermediate encoding. Through regularization terms, we encourage this encoding to both mimic the classifier’s output and also serve as the time activations of a pre-learned NMF dictionary.

FLINT and other related approaches in concept representation and their applicability for audio interpretations. FLINT represents concepts by a dictionary of attribute functions over input space. The learnt concepts are not obviously comprehensible to a user, requiring a separate visualization pipeline to get insights. Approaches based on TCAV [21], such as ACE [15], ConceptSHAP [43], define concept using a set of images and learn a representation for it in terms of hidden layers of the network, termed as concept activation vector (CAV). These designs for concepts are not related to our NMF-inspired dictionary representation. Importantly, none of the above mentioned approaches can generate listenable interpretations which is key for understandability of audio processing networks.

NMF for audio has been widely used for numerous tasks ranging from separation to transcription [38, 40, 11, 6]. Its traditional usage as a supervised dictionary or feature learning method involves learning class-wise dictionaries over training data [12]. Time activations, which are the so-called features, are generated for any data point by projecting it onto the learnt dictionaries. Extracted features can subsequently be used for downstream tasks such as classification. Bisot et al. [7] couple NMF-based features with neural networks to boost performance of acoustic scene classification.

NMF has also been successfully employed with audio–visual deep learning models for separation [13] and classification [32]. Another line of research explored unfolding iterations of different NMF optimization algorithms as a deep neural network [23, 41]. These systems, commonly known as Deep NMF, have primarily been used for audio source separation tasks.

While these works share with us the idea of combining neural networks and NMF, there is no overlap between our goals and methodologies. Unlike aforementioned studies, we wish to investigate a classifier’s decision in a post-hoc manner using NMF as a regularizer. Furthermore, to our best knowledge, attempting to regress temporal activations of a fixed NMF dictionary by accessing intermediate layers of an audio classification network is novel even within the NMF literature.

3 System Design

We begin this section with a brief note on data notation and NMF. Subsequently, in Sec. 3.1, we discuss interpreter module’s design and learning. This is followed by a description of our interpretation generation methodology in Sec. 3.2. An overview of the proposed system is presented in Fig. 1.

Data notation. We denote a training dataset by $\mathcal{S} := (x, y)_{i=1}^N$, where x is the time domain audio signal and y , a label vector. The label vector could be a one-hot or binary encoding depending upon a multi-class or multi-label dataset, respectively. Since multiple audio representations are used in this paper, a note on their notation is in order. Very often, audio signals are processed in the frequency domain through a short-time Fourier transform (STFT) on x called spectrogram. Log-mel spectrograms are a popular input to audio classification networks [33], which is also the one we use in this paper. To keep notation simple, we refer to input of the network with x . For NMF however, we favor a representation of x that can be easily inverted back to the time-domain and use a log–magnitude

spectrogram \mathbf{X} that is computed by applying an element-wise transformation $x_0 \rightarrow \log(1 + x_0)$ on the magnitude spectrogram. This is preferred over using magnitude spectrograms as it corresponds more closely to human perception of sound intensity [17].

NMF basics. NMF is a popular technique for unsupervised decomposition of audio signals [3]. Given any positive time–frequency representation $\mathbf{X} \in \mathbb{R}_+^{F \times T}$ consisting of F frequency bins and T time frames, NMF decomposes it into a product of two non-negative matrices, such that,

$$\mathbf{X} \approx \mathbf{W}\mathbf{H}$$

Here, $\mathbf{W} = [\mathbf{w}_1, \mathbf{w}_2, \dots, \mathbf{w}_K] \in \mathbb{R}_+^{F \times K}$ is interpreted as the spectral pattern or dictionary matrix containing K components and $\mathbf{H} = [\mathbf{h}_1, \mathbf{h}_2, \dots, \mathbf{h}_K]^\top \in \mathbb{R}_+^{K \times T}$ a matrix containing the corresponding time activations. Typically, a β -divergence measure between \mathbf{X} and $\mathbf{W}\mathbf{H}$ is minimized and multiplicative updates are used for estimating \mathbf{W} and \mathbf{H} [25]. Note that it is possible to reconstruct signal corresponding to each or a group of spectral components. This is typically done using a procedure called soft–masking. For a single component k , this is written as,

$$\mathbf{X}_k = \frac{\mathbf{w}_k \mathbf{h}_k^\top}{\mathbf{W}\mathbf{H}} \odot \mathbf{X}$$

Both $./$ and \odot are element-wise operations. If \mathbf{X} is an invertible representation of the magnitude spectrogram, time domain signal for \mathbf{X}_k is easily recovered using the inverse STFT operation. We extensively utilize this procedure for generating listenable interpretations. NMF can also be used for dictionary learning, by estimating \mathbf{W} on a training dataset matrix $\mathbf{X}_{\text{train}}$. As discussed later, we use a variant of NMF called Sparse-NMF [24] to pre-learn dictionary for subsequent usage in the interpretation module.

3.1 Interpreter Design

As depicted in Fig. 1 the interpreter module \mathcal{I} contains two components: an interpreter network and a NMF dictionary decoder. The so-called interpreter network computes the following function $x \mapsto \Theta \circ \Psi \circ f_{\mathcal{I}}(x)$ where Ψ is the function responsible for generating an intermediate encoding from hidden layer representations of the classification network, and Θ attempts to mimic the classifier’s output given the intermediate representation. The NMF decoder based on a pre-trained dictionary plays two roles: (i) during training, it constrains the intermediate representation to correspond to time activations of a pre-learned spectral pattern dictionary and (ii) when interpreting a classifier’s prediction, it is used to build listenable interpretation. To the best of our knowledge, this is an original usage of NMF that allows us to interpret a network’s decisions in terms of a fixed dictionary.

Design of Ψ . The function Ψ processes outputs of a set of hidden layers of the classifier, given by $f_{\mathcal{I}}(x)$. Its output, $\Psi(f_{\mathcal{I}}(x)) \in \mathbb{R}_+^{K \times T}$ produces an intermediate encoding of the interpreter. For simplicity, we will denote this intermediate encoding as $\mathbf{H}_{\mathcal{I}}(x) = \Psi \circ f_{\mathcal{I}}(x)$, a function over input x .

In practice, Ψ is modelled as a neural network that takes as input convolutional feature maps from different layers of f . To concatenate and perform joint processing on them, each feature map is first appropriately transformed to ensure same width and height dimensions. Two important aspects were kept in mind while designing subsequent layers of Ψ . Firstly, audio feature maps for spectrogram-like inputs naturally contain the notion of time and frequency along the width and height dimensions. Secondly, through appropriate regularization we wish to produce an intermediate encoding that also serves as time activations of the pre-learned NMF dictionary, a matrix of dimensions $K \times T$. To achieve this, we continuously downsample on the frequency axis and upsample the time axis to T frames. Similarly, the number of input feature maps is re-sampled to reach a size of K , equal to the number of components in dictionary \mathbf{W} . All learnable parameters of Ψ are denoted by V_Ψ .

Design of Θ . $\mathbf{H}_{\mathcal{I}}(x)$, the intermediate encoding output by Ψ is then fed to Θ , which aims to mimic output of the classifier. This directly helps in learning a representation which can interpret $f(x)$. Its design consists of two parts. The first part pools activations $\mathbf{H}_{\mathcal{I}}(x)$ across time. While this pooling can be implemented in multiple ways, we opt for attention–based pooling [20], *i.e.*, $\mathbf{z} = \sum_{t=1}^T \mathbf{H}_{\mathcal{I}}(x) \mathbf{a}_t$, where $\mathbf{a}_t \in \mathbb{R}^T$ are the attention weights and $\mathbf{z} \in \mathbb{R}^K$ is the pooled vector. The pooled representation vector is passed through a linear layer. This is followed by an appropriate activation function to convert its output to probabilities, that is, softmax for multi-class classification and sigmoid for multi-label classification. All learnable parameters of Θ are denoted by V_Θ .

174 **Fidelity loss.** Generalized cross-entropy between interpreter’s output $\Theta(\mathbf{H}_{\mathcal{I}}(x))$ and classifier’s
 175 output $f(x)$ is minimized to encourage interpreter to mimic the classifier. For multi-class classification
 176 this loss function is written as,

$$\mathcal{L}_{\text{FID}}(x, V_{\Psi}, V_{\Theta}) = -f(x)^{\top} \log(\Theta(\mathbf{H}_{\mathcal{I}}(x))) \quad (1)$$

177 On the other hand, for multi-label classification this loss reads,

$$\mathcal{L}_{\text{FID}}(x, V_{\Psi}, V_{\Theta}) = -\sum f(x) \odot \log(\Theta(\mathbf{H}_{\mathcal{I}}(x))) + (1 - f(x)) \odot \log(1 - \Theta(\mathbf{H}_{\mathcal{I}}(x))). \quad (2)$$

178 Here \odot denotes element-wise multiplication.

179 **NMF dictionary decoder and regularization.** We additionally constrain the intermediate encoding,
 180 such that, when fed to a decoder it is able to reconstruct the input audio. As already discussed, we
 181 choose this decoder to be a pre-learned NMF dictionary, \mathbf{W} . Formally, through \mathcal{L}_{NMF} we require
 182 $\mathbf{H}_{\mathcal{I}}(x)$ to approximate log-magnitude spectrogram \mathbf{X} of input audio x as $\mathbf{X} \approx \mathbf{W}\mathbf{H}_{\mathcal{I}}(x)$:

$$\mathcal{L}_{\text{NMF}}(x, V_{\Psi}) = \|\mathbf{X} - \mathbf{W}\mathbf{H}_{\mathcal{I}}(x)\|_2^2. \quad (3)$$

183 This allows us to consider $\mathbf{H}_{\mathcal{I}}(x)$ as a time activation matrix for \mathbf{W} .

184 **Training loss.** In addition to \mathcal{L}_{FID} and \mathcal{L}_{NMF} , we impose ℓ_1 regularization on $\mathbf{H}_{\mathcal{I}}(x)$ to encourage
 185 well-behavedness, especially for large dictionary sizes [24]. The complete training loss function over
 186 our training dataset \mathcal{S} can thus be given as:

$$\mathcal{L}(V_{\Psi}, V_{\Theta}) = \sum_{x \in \mathcal{S}} \mathcal{L}_{\text{FID}}(x, V_{\Psi}, V_{\Theta}) + \alpha \mathcal{L}_{\text{NMF}}(x, V_{\Psi}) + \beta \|\mathbf{H}_{\mathcal{I}}(x)\|_1 \quad (4)$$

187 where $\alpha, \beta \geq 0$ are loss hyperparameters. All the parameters of the system are constituted in the
 188 functions Ψ, Θ and dictionary \mathbf{W} . Since \mathbf{W} is pre-learned and fixed, the training loss \mathcal{L} is optimized
 189 only w.r.t V_{Ψ}, V_{Θ} . As a reminder, when training the interpreter for post-hoc analysis, the classifier
 190 network is kept fixed.

Algorithm 1 Learning algorithm

- 1: **Input:** Classifier f , Training data \mathcal{S} , parameters $V = \{V_{\Psi}, V_{\Theta}\}$, hyperparameters $\{\alpha, \beta, \mu\}$,
 number of batches B , number of training epochs N_{epoch}
 - 2: $\mathbf{W} \leftarrow \text{PRE-LEARN NMF DICTIONARY}(\mathcal{S}, \mu)$ {// Sparse-NMF algorithm}
 - 3: Random initialization of parameters V_0
 - 4: $\hat{V} \leftarrow \text{TRAIN}(f, \mathcal{S}, \mathbf{W}, V_0, \alpha, \beta, B, N_{\text{epoch}})$ {// Train with \mathcal{L} in Eq. 4}
 - 5: **Output:** $\hat{V} = \{\hat{V}_{\Psi}, \hat{V}_{\Theta}\}$
-

191 **Learning algorithm.** The complete learning pipeline is presented in Algorithm 1. The learnable
 192 parameters of the interpreter module are given by $V = \{V_{\Psi}, V_{\Theta}\}$. The pre-specified dictionary (Step
 193 2 in Algorithm 1) is learnt using Sparse-NMF [24]. The reader is referred to supplement Sec. A.1.1
 194 for more details regarding Sparse-NMF optimization problem and its application in our experiments.

195 3.2 Interpretation generation

196 Finally, to generate audio that interprets the classifier’s decision for a sample x and a predicted class
 197 c , we follow a two-step procedure: The first step consists of selecting the components which are
 198 considered “important” for the prediction. This is determined by estimating their relevance using
 199 the pooled time activations in Θ and the weights for linear layer, and then thresholding it. Precisely,
 200 given a sample x , the pooled activations are computed as $\mathbf{z} = \sum_{t=1}^T \mathbf{H}_{\mathcal{I}}(x) \mathbf{a}$. Denoting the weights
 201 for class c in the linear layer as $\theta_{c,k}^w$, the relevance of component k is estimated as $r_{k,c,x} = \frac{(\mathbf{z}_k \theta_{c,k}^w)}{\max_t |\mathbf{z}_t \theta_{c,t}^w|}$.
 202 This is essentially the normalized contribution of component k in the output logit for class c . Given a
 203 threshold τ , the selected set of components are computed as $L_{c,x} = \{k : r_{k,c,x} > \tau\}$.

204 The second step consists of estimating a time domain signal for each relevant component $k \in L_{c,x}$
 205 and also for set $L_{c,x}$ as a whole. In this paper, we refer to the latter as the generated interpretation
 206 audio, x_{int} . For certain classes, it may also be meaningful to listen to each individual component, x_k .
 207 As discussed earlier under NMF basics, estimating time domain signals from spectral patterns and
 208 their activations typically involves a soft-masking and inverse STFT procedure. We detail this step
 209 with appropriate equations in Algorithm 2.

Algorithm 2 Audio interpretation generation

```
1: Input: log-magnitude spectrogram  $\mathbf{X}$ , input phase  $\mathbf{P}_x$  components  $\mathbf{W} = \{\mathbf{w}_1, \dots, \mathbf{w}_K\}$ , time
   activations  $\mathbf{H}_{\mathcal{I}}(x) = [\mathbf{h}_1^{\mathcal{I}}(x), \dots, \mathbf{h}_K^{\mathcal{I}}(x)]^{\top}$ , set of selected components  $L_{c,x} = \{k_1, \dots, k_B\}$ .
2: for all  $k \in L_{c,x}$  do
3:    $\mathbf{X}_k \leftarrow \frac{\mathbf{w}_k \mathbf{h}_k^{\mathcal{I}}(x)^{\top}}{\sum_{l=1}^K \mathbf{w}_l \mathbf{h}_l^{\mathcal{I}}(x)^{\top}} \odot \mathbf{X}$  {// Soft masking}
4:    $x_k = \text{INV}(\mathbf{X}_k, \mathbf{P}_x)$  {// Inverse STFT}
5: end for
6:  $\mathbf{X}_{\text{int}} \leftarrow \sum_{k \in L_{c,x}} \mathbf{X}_k$ 
7:  $x_{\text{int}} = \text{INV}(\mathbf{X}_{\text{int}}, \mathbf{P}_x)$ 
8: Output:  $\{x_{k_1}, \dots, x_{k_B}\}, x_{\text{int}}$ 
```

210 4 Experiments

211 We experiment with two popular audio event analysis benchmarks, namely ESC-50 [34] and SONYC-
212 UST [9]. While the former is a multiclass environmental sound classification dataset, the latter
213 appeared for DCASE 2019 and 2020 multi-label urban sound tagging task. We quantitatively and
214 qualitatively evaluate different aspects of our interpretations, including a subjective evaluation carried
215 out on SONYC-UST. This section is organized as follows: quantitative metrics and baselines are
216 discussed in Sec. 4.1 followed by implementation details in Sec. 4.2. Experiments on ESC-50 and
217 SONYC-UST are detailed in Sec. 4.3 and Sec. 4.4, respectively.

218 4.1 Quantitative metrics and baselines

219 **Metrics.** We quantitatively evaluate our interpretations in two ways. First, by evaluating how well it
220 agrees with the classifier’s output. For multi-class classification, this is done by computing fraction
221 of samples where the class predicted by f is among the top- k classes predicted by the interpreter. We
222 refer to this as the *top- k fidelity*. To compute *fidelity* on multi-label classification tasks, we compute
223 Area Under Precision-Recall Curve (AUPRC) based metrics between the classifier output $f(x)$ and its
224 approximation by interpreter $\Theta(\mathbf{H}_{\mathcal{I}}(x))$. We compute macro-AUPRC, micro-AUPRC. Additionally,
225 we report the maximum micro F1-score over different thresholds for the interpreter’s output.

226 We also conduct a *faithfulness* evaluation for our interpretations. In general for any interpretability
227 method, *faithfulness* tries to assess if the features identified to be of high relevance are *truly* important
228 in classifier’s prediction [1]. Since a “ground-truth” importance measure for features is rarely
229 available, attribution based methods evaluate faithfulness by performing feature removal (generally
230 by setting feature value to 0) and observing the change in classifier’s output [1]. However, it is
231 hard to conduct such evaluation for non-attribution or concept based interpretation methods on data
232 modalities like image/audio, as simulating feature removal from input is not evident in these cases.

233 Interestingly, our interpretation module design allows us to simulate removal of a set of components
234 from the input. Given any sample x with predicted class c , we remove the set of relevant components
235 $L_{c,x} = \{k : r_{k,c,x} > \tau\}$ by creating a new time domain signal $x_2 = \text{INV}(\mathbf{X}_2, \mathbf{P}_x)$, where
236 $\mathbf{X}_2 = \mathbf{X} - \sum_{l \in L_{c,x}} \mathbf{X}_l$. We define faithfulness of the interpretation to classifier f for sample x with:

$$237 \text{FF}_x = f(x)_c - f(x_2)_c \quad (5)$$

238 where $f(x)_c, f(x_2)_c$ denote the output probabilities for class c . For multi-class datasets, we opt for
239 measuring absolute drop in logit value instead of absolute drop in probability. This is because class
240 probabilities are also affected by changes in logit values for other classes. It should be noted that
241 this strategy to simulate removal may introduce artifacts in the input that can affect the classifier’s
242 output unpredictably. Also, interpretations on samples with poor fidelity can lead to negative FF_x .
243 Both of these observations point to the potential instability and outlying values for this metric. Thus,
244 we report the final faithfulness of the system as median of FF_x over test set, denoted by $\text{FF}_{\text{median}}$. A
245 positive $\text{FF}_{\text{median}}$ would signify that interpretations generally tend to be faithful to the classifier.

246 **Evaluated systems.** We denote our proposed Listen to Interpret (L2I) system, with attention based
247 pooling in Θ by L2I + Θ_{ATT} . The most suitable baselines to benchmark its fidelity are *post-hoc*
248 methods that approximate the classifier over input space with a single surrogate model. We select

System	Fidelity (in %)			System	Threshold τ	FF _{median}
	top-1	top-3	top-5			
L2I + Θ_{ATT}	65.7 \pm 2.8	81.8 \pm 2.2	88.2 \pm 1.7	L2I + Θ_{ATT}	$\tau = 0.9$	0.21
L2I + Θ_{MAX}	73.3 \pm 2.3	87.8 \pm 1.8	92.7 \pm 1.2		$\tau = 0.7$	0.42
FLINT [31]	73.5 \pm 2.3	89.1 \pm 0.4	93.4 \pm 0.9		$\tau = 0.5$	0.89
VIBI [4]	27.7 \pm 2.3	45.4 \pm 2.2	53.0 \pm 1.8		$\tau = 0.3$	1.29
				Random Baseline	$\tau = 0.3$	0.00

Table 1: Quantitative results on ESC-50 environmental sound classification test data. (Left) top- k fidelity (in %). FLINT and VIBI help benchmark fidelity but are not themselves suitable for audio interpretations. (Right) Faithfulness results (absolute drop in logit value) for different thresholds, τ . We report FF_{median} for proposed L2I + Θ_{ATT} and the Random Baseline.

two state-of-the-art systems, FLINT [31] and VIBI [4]. A variant of our own proposed method, L2I + Θ_{MAX} , is also evaluated. Herein, attention is replaced with 1D max-pooling operation. Implementation details of the baselines are discussed in supplement Sec. A.1.6.

Faithfulness benchmarking: As already discussed, it is not possible to measure faithfulness for concept-based *post-hoc* interpretability approaches. While measurement for input attribution based approaches is possible, the interpretations themselves and the feature removal strategies are different, making comparisons with our system significantly less meaningful. We thus compare our faithfulness against a *Random Baseline*, wherein the less-important components, those not present in $L_{c,x}$, are randomly removed. To compare fairly, we remove the same number of components that are present in $L_{c,x}$ on average. This would validate that, if the interpreter selects *truly* important components for the classifier’s decision, then randomly removing the less important ones should not cause a drop in the predicted class probability/logit.

We also emphasize at this point that works related to audio interpretability (see Sec. 2), are not suitable for comparison on these metrics. Particularly, APNet [45] is not designed for *post-hoc* interpretations. AudioLIME [18] is not applicable on our tasks as it requires known predefined audio sources. Moreover, SLIME [29] and AudioLIME still rely on LIME [35] for interpretations. It is a feature-attribution method that approximates a classifier for *each* sample separately. As discussed before, these characteristics are not suitable for comparison on our metrics.

4.2 Implementation details

Classification network. We interpret a VGG-style convolutional neural network proposed by Kumar et al. [22]. This network was chosen due to its popularity and applicability for various audio scene and event classification tasks. It can process variable length audio and has been pretrained on AudioSet [14], a large-scale weakly labeled dataset for sound events. Further details about the network and its fine-tuning can be found in supplement Sec. A.1.2.

Hyperparameters and training. The hidden layers input to the interpreter module are selected from the convolutional block outputs. As is often the case with CNNs, the latter layers are expected to capture higher-order features. We thus select the last three convolutional block outputs as input to the network Ψ . For ESC-50, we pre-learn the dictionary \mathbf{W} with $K = 100$ components and for SONYC-UST, we learn with $K = 80$ components. Reasons for choice of K are discussed in supplement Sec. A.1.3. Ablation studies for other hyperparameters are in supplement Sec. A.1.4.

4.3 Experiments on ESC-50

Dataset. ESC-50 [34] is a popular benchmark for environmental sound classification task. It is a multi-class dataset that contains 2000 audio recordings of 50 different environmental sounds. The classes are broadly arranged in five categories namely, animals, natural soundscapes/water sounds, human/non-speech sounds, interior/domestic sounds, exterior/urban noises. Each clip is five-seconds long and has been extracted from publicly available recordings on the `freesound.org` project. The dataset is prearranged into 5 folds.

Classifier performance. The classifier achieves an accuracy of $82.5 \pm 1.9\%$ over the 5 folds, higher than the average human accuracy of 81.3% on ESC-50.

Quantitative results. Mean and standard deviation of top- k fidelity is calculated over the 5 folds. We show these results in Table 1 (Left) for $k = 1, 3, 5$. Among the four systems, VIBI performs the worst in terms of fidelity. This is very likely because it treats the classifier as a black-box, while the other three systems access its hidden representations. This strongly indicates that accessing hidden layers can be beneficial for fidelity of interpreters. FLINT achieves the highest fidelity, very closely followed by $L2I + \Theta_{MAX}$ and then $L2I + \Theta_{ATT}$. This experiment serves as a sanity check for our system, that while achieving fidelity performance comparable to state-of-the-art, we hold the advantage of providing listenable interpretations in terms of pre-learned spectral patterns.

In Table 1 (Right), we report median faithfulness FF_{median} (absolute drop in logit value) on fold-1 for our primary system $L2I + \Theta_{ATT}$ at different thresholds τ . Smaller τ corresponds to higher $|L_{c,x}|$, which denotes the number of components being used for generating interpretations. Thus, for Random Baseline, we report FF_{median} at the lowest threshold $\tau = 0.3$, to ensure removal of maximal number of components. To recall the definition of Random Baseline, please refer to Sec. 4.1. FF_{median} for $L2I + \Theta_{ATT}$ is positive for all thresholds. It is also significantly higher than the Random Baseline, indicating faithfulness of interpretations.

Audio corruption experiment: an interpretability illustration. We qualitatively illustrate that the interpretations are capable of emphasizing the object of interest and are insightful for an end-user to understand the classifier’s prediction. To do so, we generate interpretations after corrupting the testing data for fold-1 in two different ways (i) either with white noise at 0dB SNR (signal-to-noise ratio), (ii) or mixing it with sample of different class. It should be noted that in both these cases the system is exactly the same as before and **not** trained with corrupted samples. Some examples, covering both types of corruptions are shared on our companion website.¹. A detailed qualitative analysis of this experiment can be found in supplement Sec. A.1.5.

4.4 Experiments on SONYC-UST

We now discuss experiments for the urban sound tagging task from the well known Detection and Classification of Acoustic Scenes and Events (DCASE) challenge 2019 & 2020 edition.

Dataset. The DCASE task used a very challenging real-world dataset called SONYC-UST [8]. It contains audio collected from multiple sensors placed in the New York City to monitor noise pollution. It consists of eight coarse-level and 20 fine-level labels. We opt for the coarse-level labeling task that involves multi-label classification into: ‘engine’, ‘machinery-impact’, ‘non-machinery-impact’, ‘powered-saw’, ‘alert-signals’, ‘music’, ‘human-voice’, ‘dog’. This task is highly challenging for several reasons: (i) since it is real-world audio, the samples contain a very high level of background noise, (ii) the audio sources corresponding to the classes are often weak in intensity, as they are not necessarily close to the sensors, (iii) some classes may also be highly localized in time and more challenging to detect, (iv) lastly, noisy audio also makes it difficult to annotate, leading to labeling noise. This is especially true for training data that was labeled by volunteers.

Classifier performance. Our fine-tuned classifier achieves a macro-AUPRC (official metric for DCASE 2020 challenge) of 0.601. This is higher than the DCASE baseline performance of 0.510 and comparable to the best performing system macro-AUPRC of 0.649 [2]. Note that it is obtained without use of data augmentation or additional strategies to improve performance.

Quantitative results. In Table 2, we report the macro-AUPRC, micro-AUPRC and max-F1 for the interpreter output w.r.t classifier. For fairness, we ignore the class ‘non-machinery impact’ from all class-wise evaluations involved in fidelity (*i.e.* macro-AUPRC) or faithfulness. This is because the classifier predicts only one sample in test set with positive label for this class, causing AUPRC scores to vary widely for different interpreters. VIBI has the worst performance on all three metrics for this dataset as well. In contrast to ESC-50, here the best performing system is $L2I + \Theta_{ATT}$ followed by $L2I + \Theta_{MAX}$, and FLINT performing worse than both. The fidelity results on ESC-50 and SONYC-UST jointly demonstrate that our interpreter can generate high-fidelity *post-hoc* interpretations. Moreover, its design is flexible w.r.t different pooling functions.

The results for class-wise faithfulness are illustrated in Fig. 2a. We show FF_{median} (absolute drop in probability) for our system and the Random Baseline. The results indicate that, for most classes, interpretations can be considered faithful, with a significantly positive median compared to random baseline results, which are very close to 0.

¹<https://listen2interpret.000webhostapp.com/>

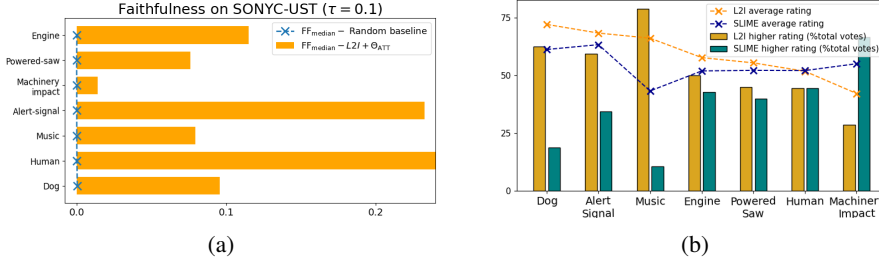


Figure 2: (a) Faithfulness (absolute drop in probability value) results for SONYC-UST arranged class-wise for threshold, $\tau = 0.1$ (b) Subjective evaluation results. Average scores for L2I and SLIME and fraction of votes in favour of each system are reported.

System	Fidelity		
	macro-AUPRC	micro-AUPRC	max-F1
$L2I + \Theta_{ATT}$	0.909 ± 0.011	0.917 ± 0.008	0.847 ± 0.010
$L2I + \Theta_{MAX}$	0.866 ± 0.014	0.913 ± 0.012	0.840 ± 0.012
FLINT	0.816 ± 0.013	0.907 ± 0.011	0.825 ± 0.012
VIBI	0.608 ± 0.027	0.575 ± 0.019	0.549 ± 0.020

Table 2: Fidelity results on SONYC-UST multi-label urban sound tagging task. We report AUPRC-based metrics and max F1 score for the interpreter w.r.t classifier’s output (over three runs).

Qualitative observations. Qualitatively, we observe good interpretations for classes ‘alert-signal’, ‘dog’ and ‘music’. For them, the background noise is significantly suppressed and the interpretations mainly focus on the object of interest. Interpretations for class ‘human’ are also able to suppress noise to a certain extent and focus on parts of human voices. However, for this class, we found presence of some signal from other audio sources too. For the remaining classes, namely ‘Engine’, ‘Powered-saw’ and ‘Machinery-impact’ the quality of the interpretation is more sample dependent. This is due to their acoustic similarity with the background noise. We provide example interpretations for SONYC-UST on our companion website.¹ We present an additional visualization to demonstrate coherence of our interpretations in supplement Sec. A.1.5.

Subjective evaluation. We perform a user study (15 participants) to evaluate quality and understandability of interpretations for L2I against SLIME on SONYC-UST test data. As discussed in Sec. 4.1, SLIME is not suitable for comparison on our quantitative metrics. Nevertheless, it is the only relevant baseline for qualitative study of listenable interpretations. Details about SLIME implementation are in supplement Sec. A.1.6. A participant was provided with 10 input samples, a predicted class by the classifier for each sample and the corresponding interpretation audios from SLIME and L2I. They were asked to rate the interpretations on a scale of 0-100 for the following question: “How well does the interpretation correspond to the part of input audio associated with the given class?”. The 10 samples were randomly selected from a set of 36 (5-6 random test examples per class). For each sample, we ensured that the predicted class was both, present in the ground-truth and audible in input. Class-wise preference results and average ratings are shown in Fig. 2b. L2I is preferred for ‘music’, ‘dog’ & ‘alert-signal’, SLIME is preferred for ‘machinery-impact’, no clear preference for others.

5 Conclusion

To sum up, we have presented a system for post-hoc interpretation of networks that process audio. We posit that generating interpretations in terms of high-level audio objects and making them listenable are important attributes to aid understanding. Novel usage of NMF within our interpreter helps us satisfy both aforementioned requirements. Our original loss function formulation enables linking a classifier’s decision to importance values over pre-learned NMF spectral dictionary through an intermediate encoding. We perform extensive evaluation over popular audio event analysis datasets. We present a first-of-its-kind faithfulness evaluation for our non-attribution based method. Finally, a user study confirms usefulness of our listenable interpretations. Modular design of our system calls for further experimenting with decoder and other block architectures. We hope our work facilitates future research into designing modality-specific interpreters that aid understanding.

Checklist

1. For all authors...

- (a) Do the main claims made in the abstract and introduction accurately reflect the paper’s contributions and scope? [Yes]
- (b) Did you describe the limitations of your work? [Yes] See supplement Sec. A.1.8
- (c) Did you discuss any potential negative societal impacts of your work? [N/A] We discuss potential societal impacts in supplement Sec. A.1.8
- (d) Have you read the ethics review guidelines and ensured that your paper conforms to them? [Yes]

2. If you are including theoretical results...

- (a) Did you state the full set of assumptions of all theoretical results? [N/A]
- (b) Did you include complete proofs of all theoretical results? [N/A]

3. If you ran experiments...

- (a) Did you include the code, data, and instructions needed to reproduce the main experimental results (either in the supplemental material or as a URL)? [Yes]
- (b) Did you specify all the training details (e.g., data splits, hyperparameters, how they were chosen)? [Yes]
- (c) Did you report error bars (e.g., with respect to the random seed after running experiments multiple times)? [Yes]
- (d) Did you include the total amount of compute and the type of resources used (e.g., type of GPUs, internal cluster, or cloud provider)? [Yes]

4. If you are using existing assets (e.g., code, data, models) or curating/releasing new assets...

- (a) If your work uses existing assets, did you cite the creators? [Yes]
- (b) Did you mention the license of the assets? [Yes]
- (c) Did you include any new assets either in the supplemental material or as a URL? [N/A]
- (d) Did you discuss whether and how consent was obtained from people whose data you’re using/curating? [N/A] All assets are free and public for research
- (e) Did you discuss whether the data you are using/curating contains personally identifiable information or offensive content? [N/A]

5. If you used crowdsourcing or conducted research with human subjects...

- (a) Did you include the full text of instructions given to participants and screenshots, if applicable? [Yes] Please see supplement Sec. A.1.7
- (b) Did you describe any potential participant risks, with links to Institutional Review Board (IRB) approvals, if applicable? [N/A]
- (c) Did you include the estimated hourly wage paid to participants and the total amount spent on participant compensation? [N/A] It was optional for participants

References

- [1] David Alvarez-Melis and Tommi Jaakkola. Towards robust interpretability with self-explaining neural networks. In *Advances in Neural Information Processing Systems (NeurIPS)*, pages 7775–7784, 2018.
- [2] Augustin Arnault and Nicolas Riche. CRNNs for urban sound tagging with spatiotemporal context. Technical report, DCASE2020 Challenge, October 2020.
- [3] Roland Badeau and Tuomas Virtanen. Nonnegative matrix factorization. *Audio Source Separation and Speech Enhancement*, pages 131–160, 2018.
- [4] Seojin Bang, Pengtao Xie, Heewook Lee, Wei Wu, and Eric Xing. Explaining a black-box by using a deep variational information bottleneck approach. In *Proceedings of the AAAI Conference on Artificial Intelligence*, volume 35, pages 11396–11404, 2021.

- 421 [5] Sören Becker, Marcel Ackermann, Sebastian Lapuschkin, Klaus-Robert Müller, and Wojciech
422 Samek. Interpreting and explaining deep neural networks for classification of audio signals.
423 *arXiv preprint arXiv:1807.03418*, 2018.
- 424 [6] Nancy Bertin, Roland Badeau, and Gaël Richard. Blind signal decompositions for automatic
425 transcription of polyphonic music: Nmf and k-svd on the benchmark. In *2007 IEEE Interna-*
426 *tional Conference on Acoustics, Speech and Signal Processing-ICASSP'07*, volume 1, pages
427 I–65. IEEE, 2007.
- 428 [7] Victor Bisot, Romain Serizel, Slim Essid, and Gaël Richard. Feature learning with matrix
429 factorization applied to acoustic scene classification. *IEEE/ACM Transactions on Audio, Speech,*
430 *and Language Processing*, 25(6):1216–1229, 2017.
- 431 [8] Mark Cartwright, Ana Elisa Mendez Mendez, Jason Cramer, Vincent Lostanlen, Graham Dove,
432 Ho-Hsiang Wu, Justin Salamon, Oded Nov, and Juan Bello. SONYC urban sound tagging
433 (SONYC-UST): A multilabel dataset from an urban acoustic sensor network. In *Proceedings of*
434 *the Workshop on Detection and Classification of Acoustic Scenes and Events (DCASE)*, pages
435 35–39, October 2019.
- 436 [9] Mark Cartwright, Jason Cramer, Ana Elisa Mendez Mendez, Yu Wang, Ho-Hsiang Wu, Vin-
437 cent Lostanlen, Magdalena Fuentes, Graham Dove, Charlie Mydlarz, Justin Salamon, et al.
438 Sonyc-ust-v2: An urban sound tagging dataset with spatiotemporal context. *arXiv preprint*
439 *arXiv:2009.05188*, 2020.
- 440 [10] Shreyan Chowdhury, Verena Praher, and Gerhard Widmer. Tracing back music emotion
441 predictions to sound sources and intuitive perceptual qualities. *arXiv preprint arXiv:2106.07787*,
442 2021.
- 443 [11] Christian Dittmar and Daniel Gärtner. Real-time transcription and separation of drum recordings
444 based on nmf decomposition. In *DAFx*, pages 187–194, 2014.
- 445 [12] Cédric Févotte, Emmanuel Vincent, and Alexey Ozerov. Single-channel audio source separation
446 with nmf: divergences, constraints and algorithms. *Audio Source Separation*, pages 1–24, 2018.
- 447 [13] Ruohan Gao, Rogerio Feris, and Kristen Grauman. Learning to separate object sounds by
448 watching unlabeled video. In *Proceedings of the European Conference on Computer Vision*
449 *(ECCV)*, pages 35–53, 2018.
- 450 [14] Jort F Gemmeke, Daniel PW Ellis, Dylan Freedman, Aren Jansen, Wade Lawrence, R Channing
451 Moore, Manoj Plakal, and Marvin Ritter. Audio set: An ontology and human-labeled dataset
452 for audio events. In *2017 IEEE International Conference on Acoustics, Speech and Signal*
453 *Processing (ICASSP)*, pages 776–780. IEEE, 2017.
- 454 [15] Amirata Ghorbani, James Wexler, James Y Zou, and Been Kim. Towards automatic concept-
455 based explanations. In *Advances in Neural Information Processing Systems (NeurIPS)*, pages
456 9277–9286, 2019.
- 457 [16] Leilani H Gilpin, David Bau, Ben Z Yuan, Ayesha Bajwa, Michael Specter, and Lalana Kagal.
458 Explaining explanations: An overview of interpretability of machine learning. In *2018 IEEE*
459 *5th International Conference on data science and advanced analytics (DSAA)*, pages 80–89.
460 IEEE, 2018.
- 461 [17] JL Goldstein. Auditory nonlinearity. *The Journal of the Acoustical Society of America*, 41(3):
462 676–699, 1967.
- 463 [18] Verena Haunschmid, Ethan Manilow, and Gerhard Widmer. audiolime: Listenable explanations
464 using source separation. *arXiv preprint arXiv:2008.00582*, 2020.
- 465 [19] Lisa Anne Hendricks, Zeynep Akata, Marcus Rohrbach, Jeff Donahue, Bernt Schiele, and
466 Trevor Darrell. Generating visual explanations. In *European Conference on Computer Vision*,
467 pages 3–19. Springer, 2016.
- 468 [20] Maximilian Ilse, Jakub Tomczak, and Max Welling. Attention-based deep multiple instance
469 learning. In *International conference on machine learning*, pages 2127–2136. PMLR, 2018.

- [21] Been Kim, Martin Wattenberg, Justin Gilmer, Carrie Cai, James Wexler, Fernanda Viegas, and Rory Sayres. Interpretability beyond feature attribution: Quantitative testing with concept activation vectors (tcav). *arXiv preprint arXiv:1711.11279*, 2017.
- [22] Anurag Kumar, Maksim Khadkevich, and Christian Fügen. Knowledge transfer from weakly labeled audio using convolutional neural network for sound events and scenes. In *2018 IEEE International Conference on Acoustics, Speech and Signal Processing (ICASSP)*, pages 326–330. IEEE, 2018.
- [23] Jonathan Le Roux, John R Hershey, and Felix Weninger. Deep nmf for speech separation. In *2015 IEEE International Conference on Acoustics, Speech and Signal Processing (ICASSP)*, pages 66–70. IEEE, 2015.
- [24] Jonathan Le Roux, Felix J Weninger, and John R Hershey. Sparse nmf–half-baked or well done? *Mitsubishi Electric Research Labs (MERL), Cambridge, MA, USA, Tech. Rep., no. TR2015-023*, 11:13–15, 2015.
- [25] Daniel Lee and H. Sebastian Seung. Algorithms for non-negative matrix factorization. In T. Leen, T. Dietterich, and V. Tresp, editors, *Advances in Neural Information Processing Systems*, volume 13. MIT Press, 2001. URL <https://proceedings.neurips.cc/paper/2000/file/f9d1152547c0bde01830b7e8bd60024c-Paper.pdf>.
- [26] AM Liberman, Franklin S Cooper, Donald P Shankweiler, and Michael Studdert-Kennedy. Why are speech spectrograms hard to read? *American Annals of the Deaf*, pages 127–133, 1968.
- [27] Scott M Lundberg and Su-In Lee. A unified approach to interpreting model predictions. In *Advances in Neural Information Processing Systems*, pages 4765–4774, 2017.
- [28] Saumitra Mishra, Bob L Sturm, and Simon Dixon. Local interpretable model-agnostic explanations for music content analysis. In *ISMIR*, pages 537–543, 2017.
- [29] Saumitra Mishra, Emmanouil Benetos, Bob LT Sturm, and Simon Dixon. Reliable local explanations for machine listening. In *2020 International Joint Conference on Neural Networks (IJCNN)*, pages 1–8. IEEE, 2020.
- [30] Grégoire Montavon, Wojciech Samek, and Klaus-Robert Müller. Methods for interpreting and understanding deep neural networks. *Digital Signal Processing*, 73:1–15, 2018.
- [31] Jayneel Parekh, Pavlo Mozharovskiy, and Florence d’Alché Buc. A framework to learn with interpretation. In *Advances in Neural Information Processing Systems (NeurIPS)*, 2021.
- [32] Sanjeel Parekh, Alexey Ozerov, Slim Essid, Ngoc QK Duong, Patrick Pérez, and Gaël Richard. Identify, locate and separate: Audio-visual object extraction in large video collections using weak supervision. In *2019 IEEE Workshop on Applications of Signal Processing to Audio and Acoustics (WASPAA)*, pages 268–272. IEEE, 2019.
- [33] Geoffroy Peeters and Gaël Richard. Deep learning for audio and music. In J. Benois-Pineau and A. Zemmari, editors, *Multi-faceted Deep Learning: Models and Data*, pages 231–266. Springer, 2021.
- [34] Karol J Piczak. Esc: Dataset for environmental sound classification. In *Proceedings of the 23rd ACM international conference on Multimedia*, pages 1015–1018, 2015.
- [35] Marco Tulio Ribeiro, Sameer Singh, and Carlos Guestrin. Why should i trust you?: Explaining the predictions of any classifier. In *Proceedings of the 22nd ACM SIGKDD international conference on knowledge discovery and data mining*, pages 1135–1144. ACM, 2016.
- [36] Marco Tulio Ribeiro, Sameer Singh, and Carlos Guestrin. Anchors: High-precision model-agnostic explanations. In *Proceedings of the AAAI Conference on Artificial Intelligence*, volume 32, 2018.
- [37] Ramprasaath R Selvaraju, Michael Cogswell, Abhishek Das, Ramakrishna Vedantam, Devi Parikh, and Dhruv Batra. Grad-cam: Visual explanations from deep networks via gradient-based localization. In *Proceedings of the IEEE International Conference on Computer Vision*, pages 618–626, 2017.

- 519 [38] Paris Smaragdis. Non-negative matrix factor deconvolution; extraction of multiple sound
520 sources from monophonic inputs. In *International Conference on Independent Component*
521 *Analysis and Signal Separation*, pages 494–499. Springer, 2004.
- 522 [39] Sana Tonekaboni, Shalmali Joshi, Kieran Campbell, David K Duvenaud, and Anna Goldenberg.
523 What went wrong and when? instance-wise feature importance for time-series black-box models.
524 *Advances in Neural Information Processing Systems*, 33:799–809, 2020.
- 525 [40] Kevin W Wilson, Bhiksha Raj, Paris Smaragdis, and Ajay Divakaran. Speech denoising
526 using nonnegative matrix factorization with priors. In *2008 IEEE International Conference on*
527 *Acoustics, Speech and Signal Processing*, pages 4029–4032. IEEE, 2008.
- 528 [41] Scott Wisdom, Thomas Powers, James Pitton, and Les Atlas. Deep recurrent nmf for speech
529 separation by unfolding iterative thresholding. In *2017 IEEE Workshop on Applications of*
530 *Signal Processing to Audio and Acoustics (WASPAA)*, pages 254–258. IEEE, 2017.
- 531 [42] Minz Won, Sanghyuk Chun, and Xavier Serra. Toward interpretable music tagging with
532 self-attention. *arXiv preprint arXiv:1906.04972*, 2019.
- 533 [43] Chih-Kuan Yeh, Been Kim, Sercan O Arik, Chun-Liang Li, Pradeep Ravikumar, and Tomas Pfister.
534 On concept-based explanations in deep neural networks. *arXiv preprint arXiv:1910.07969*,
535 2019.
- 536 [44] Jinsung Yoon, James Jordon, and Mihaela van der Schaar. Invase: Instance-wise variable
537 selection using neural networks. In *International Conference on Learning Representations*,
538 2018.
- 539 [45] Pablo Zinemanas, Martín Rocamora, Marius Miron, Frederic Font, and Xavier Serra. An
540 interpretable deep learning model for automatic sound classification. *Electronics*, 10(7):850,
541 2021.